IEEE Access
Multidisciplinary | Rapid Review | Open Access Journal

Received January 24, 2022, accepted February 13, 2022, date of publication February 17, 2022, date of current version March 4, 2022.

Digital Object Identifier 10.1109/ACCESS.2022.3152557

Novel Design of Slim Mould Optimizer for the Solution of Optimal Power Flow Problems Incorporating Intermittent Sources: A Case Study of Algerian Electricity Grid

SOUHIL MOUASSA[1,3], AHMED ALTHOBAITI[2], (Member, IEEE), FRANCISCO JURADO[3], (Senior Member, IEEE), AND SHERIF S. M. GHONEIM[2], (Senior Member, IEEE)

[1]Department of Electrical Engineering, University of Bouira, Bouira 10000, Algeria
[2]Department of Electrical Engineering, College of Engineering, Taif University, Taif 21944, Saudi Arabia
[3]Department of Electrical Engineering, University of Jaén, 23700 Jaén, Spain

Corresponding author: Souhil Mouassa (souhil.mouassa@univ-bouira.dz)

This work was supported by the Taif University Researchers Supporting Project, Taif University, Taif, Saudi Arabia, under Grant TURSP-2020/34.

ABSTRACT Nowadays, electrical power grids are facing increased penetration of renewable energy sources (RES), which result in increasing level of randomness and uncertainties for its operational quality. In addition, emerging need for efficient solutions to stochastic optimal power flow (OPF) problem has attracted considerable attention to ensure optimal and reliable grid operations in the presence of generation uncertainty and increasing demand. Therefore, this paper proposes an efficient Slime Mould-inspired Algorithm (SMA) that aims to minimize overall operating cost of main grid by managing the power flow among different generating resources. The problem is formulated as large-scale constrained optimization problem with non-linear characteristics. Its degree of complexity increases with incorporation of intermittent energy sources, making it harder to be solved using conventional optimization techniques. However, could be efficiently resolved by nature-inspired optimization techniques without any modification or approximation into the original-formulation. The objective function is the overall cost of system, including reserve cost for over-estimation and penalty cost for under-estimation of both PV-solar and wind energy. The SMA performance is evaluated on the IEEE 30-bus test system and Algerian power system, DZA 114-bus. The SMA is compared with four optimization algorithms: i) The well-studied meta-heuristics, i.e., Gorilla troops optimizer (GTO), and Orca predation algorithm (OPA), ii) Recently developed meta-heuristics, i.e., Artificial ecosystem optimizer (AEO), Hunger games search (HGS), and Jellyfish search (JS) optimizer, iii) ad high-performance meta-heuristics, Success-History based parameter adaptation for differential evolution method. The overall simulation results reveal that the SMA ranked first among the compared algorithms, and so, over and so, over different function landscapes.

INDEX TERMS Optimal power flow (OPF), emission, renewable energy sources, uncertainty, gorilla troop optimizer, orca predation algorithm, slime mould algorithm.

LIST OF ABBREVIATIONS

P_{loss}	The Total Power Losses.
TVD	Total Voltage Deviation.
δ_{ij}	The voltage angle difference between i and bus j.
q_{ji}	The phase angle of term F_{ji}.
V_{Gi}	Voltage Magnitude for Generator at Bus i.
N_{PV}	The number of PV.
N_{PQ}	The number of PQ buses (Load buses).
g_k	Conductance of k^{th} branch connected between i & j.

The associate editor coordinating the review of this manuscript and approving it for publication was Hazlie Mokhlis.

V_i, V_j	Voltage magnitude for load bus *i* & *j*.
$V_{L,N_{PQ}}$	Voltage Magnitude for Load Bus i.
$\lvert Y_{ij} \rvert$	The Elements of Bus Admittance Matrix.
S_i	Apparent Power Flow of Branch *i*.
$P_{D,i}$	Active Power Load Consumption at Bus *i*.
$Q_{D,i}$	Reactive Power Load Consumption at Bus *i*.
P_{Gi}/Q_{Gi}	Active/Reactive Power Generation at Bus *i*.
V_i^{max}	Maximum Bus Voltage Magnitude at Bus *i*.
V_i^{min}	Minimum Bus Voltage Magnitude at Bus *i*.
P_{Gi}/Q_{Gi}	Active/Reactive Power Generation at Bus *i*.
P_{Di}/Q_{Di}	Active/Reactive, Load Consumption at Bus *i*.
$P_{L,N_{PQ}}$, $Q_{L,N_{PQ}}$	Active and reactive power at each load bus.
Q_{Gi}^{min}, Q_{Gi}^{max}	Limits Value of Reactive Power Generation.
NLB	Number of Load Buses.
NG	Number of Generators Buses.
λ_V, λ_Q, λ_l	The penalty factors.
SMA	Slime Mould Algorithm.
OPA	Orca Predator Algorithm.
AEO	Artificial Ecosystem Algorithm.
GTO	Gorilla Troops Optimizer.
HGS	Hunger Games Search.
RES	Renewable Energy Sources.
TG	Thermal Generator.
WG	Wind Generator.
SG	Solar Generator.

I. INTRODUCTION

Optimal power Flow (OPF) is one of primordial tools of electric power systems, offering electric power at minimum-cost and high quality. In short, is therefore the backbone tool of electric grids due to the important role which plays to maintain reliable and economical system operation. OPF Master Objective is to specify the optimal adjustment of control variables so that a selected objective function is optimized while satisfying different physical and operational-constraints inflicted by electric power grids (equality and inequality constraints). The most commonly objective-function is minimization of overall generation cost. However, other functions are minimization of gas emission, real power loss, voltage stability-index (VSI), and bus voltage-deviation [1]. While used control-variables are: active power of generators outputs, generator voltages magnitudes, positions of the transformer taps, and contributions of the compensators in terms of reactive power. These variables are mixture between discrete and continuous ones; parallel compensators and taps changer transformer are discrete variables, while remaining ones are continuous.

In traditional electric grids, the study of OPF considers conventional power generators run on fossil-fuels. However, under electricity market liberalisation, and integration of renewable energy sources (RES), study of OPF is becoming more complicated leading in increase the complexity of its objectives significantly. This is due to the diverse functions based on the variability and uncertain used in its problem formulation. The prime objective behind incorporation of renewable generators (WT+PV) in the grids is to reduce the transmission line losses and improving the reliability and quality of electric grids. Also they reduce environmental pollution. [1] In addition, with increasing of injected power from RES, specifying optimal contribution of each generator in the system is necessity. Thus, energy management and optimal scheduling of different resources could facilitate diverse missions of electric power system operator, ultimately reducing total generation electricity cost.

In the few past decades, numerous conventional optimization techniques have been applied to solve different versions of OPF problem. The conventional solvers are the Newton method [2] [3], non-linear programming (NLP) [4] and interior point methods [5]. Despite the fact that some of abovementioned methods have excellent convergence characteristics and some of them are usually suitable for industry applications. However, they have some weaknesses, which are summarized as follows:

1) Sensitivity to the initial search point, i.e., they might converge easily to local solutions as may converge to global ones.
2) Lack of flexibility with respect to practical systems, i.e., each method is suit for a specific problem formulation in its proper objectives and/or constraints.
3) Besides the inflexibility aspect, they also encounter a huge difficult to set of uncertain and stochastic problems, such as OPF with application of renewable generation.

Therefore, developing new and effective optimization methods is necessity in effort to overcome the shortcomings of the traditional optimization techniques'. [6] Thanks to the computational intelligence schemes and open access to optimization techniques have liberated considerable researches in the field of meta-heuristic algorithms to solve complex optimization problems during first decade. These optimizers have ability to provide near-global solutions and capability to escape local ones, avoiding in premature convergence. Many meta-heuristic optimization algorithms have been implemented to cope with classical OPF problem like improved version of PSO [7], moth swarm algorithm (MSA) [8], improved bacterial forging method (IBF) [9], teaching-learning-based optimization (TLBO) technique [10], backtracking-search algorithm (BSA) [11], improved colliding-bodies optimizer (ICBO) [12], adaptive multiple teams perturbation-guiding Jaya (AMTPG-Jaya) algorithm [13], and Differential Evolution [14] While

aforementioned references are limited on the thermal power generators only. In the few past years, a system with mixed resources involving thermal, wind and solar generators have been studied in quest of provide electrical energy at minimum generation-cost with high-quality. As mentioned earlier, electricity market allows the incorporation of renewable energy sources into the electricity grids in order to minimize the environmental problems and enhancement of load relief on a transmission lines as well system voltage profile control by transmission line active power losses reduction. In that context, a few works have been published in literatures. For instance in [15] modified Jaya algorithm is applied to solve OPF incorporating RES considering four different objective functions to improve recorded results against other optimizers while the RES is modeled as a negative load, but any forecasting technique was not employed to forecast wind and solar photovoltaic power output. The results show outperforms of MJAYA on the basic Jaya as well on other existing algorithms.Partha Biswas *et al.* [16] proposed an adaptive version of differential evolution-based technique (SHADE) to solve OPF problem in a system involving renewable power generators. To forecast wind power and solar-photovoltaic production, authors used Weibull and lognormal probability-distribution-functions (PDF). In addition, the feasibility of results was discussed and checked that all control variables fell inside the allowed limits. Thus, findings clearly show the efficacy of the proposed model, but, unfortunately, it was applied only on medium-sized test system, IEEE 30-bus. In another publication [17], Ehab E.Elattar proposed modified version of the moth swarm algorithm to solve OPF problem of combined heat and power system with presence stochastic wind farm. The model is well presented and results were discussion but only for IEEE 30-bus system in which feasibility of solution of large-scale test system IEEE 118-bus were not discussed. As well, application of suggested model on a practical power grid was not conducted. Zia Ullah et al [18] provide a new hybrid optimization algorithm PPSOGSA for OPF solution considering renewable energy generators. The model of stochastic behavior is based of PDF scheme. The results amply show the superiority of proposed hybrid method against basic PPSO and GSA. Again, however, the algorithm was not examined by applying it to real/ large-sized power system. In Yu-Cheng Chang *et al.* [19], evolutionary particle swarm optimization (EPSO) algorithm was used for solving OPF problem in a wind-thermal power system. The suggested wind model is based on the up-spinning and down-spinning reserves of the production units. But, the approach was also evaluated only on modified IEEE 30-bus system and large-scale power systems were not taken into consideration when validating the proposed model. A modified cuckoo search optimization technique employed for OPF solution incorporating wind power was proposed in Chetan Mishra el al in [20]. Authors in [21] proposes a new strategy for the optimal scheduling problem taking into account the impact of uncertainties in RES and load demand forecasts. GA is used to test the effectiveness of the suggested optimal scheduling strategy by applied on the medium and large-scale test system IEEE 30-bus and 300-bus. In overall obtained results were good and promising too.

In view of aforementioned works, published results are promising and encouraging. But bear in mind that in spite of all efforts carried out in this area since half-a-century ago, topic is remains open for research and also worthy of further attention. On the other hand, despite the success of many optimization methods in realizing satisfactory results, but still suffer from some limitations and shortcomings as far as their susceptibility of falling into local optima and the difficulty of tuning the main intrinsic parameters. More precisely, none of them can guarantee finding the optimal solution for all optimization problems.

Moreover, application of these algorithms on larger scale or real-sized electric grids is uncommon. Consequently, these gaps give an opportunity to suggest or develop effective meta-heuristic techniques able deal different OPF formulations.

In this paper, a SM algorithm is proposed to deal with OPF problem in the presence RES and different objective functions. The proposed SMA is examined on the medium-test system IEEE 30-bus, and a real-sized DZA114-bus power system. In addition, superiority of feasible solutions (SF) method is used herein to handle constraints of stochastic OPF problem. Slime Mould Algorithm (SMA) is a novel stochastic optimization algorithm nature-inspired proposed by Shimin Li et *al.* in 2020 [22], which simulates the behavior of *Physarum polycephalum* and morphological changes of slime mould while searching food. Its structure is very simple, which makes it easier to implement for various optimization problems [22]. Also, it has excellent randomness properties, makes it search for all optimal solutions in the search-space, hence effectively avoiding local-optimum. In addition, the following points summarize precisely master benefits of proposed SMA and also serving as motivational factors for selecting this optimizer.

1) Adaptive variation of weight allows the SMA to keep a certain perturbation-rate while warranting fast convergence, thus preventing search-process in confined regions (local optima).
2) It has an important parameter of vibration V_b allows the individual position of SM to contract in a specific method, which guaranteeing early exploration and the accuracy of the exploitation process.
3) The position updating decision parameter DS and three different position updating schemes guarantee better capability of the SMA in different search-phases.
4) The numerical results of engineering optimization problems in real life showed that SMA is more efficiency than the compared optimization techniques.

Remainder of this paper is organized as follows. Section 2 introduces the problem definition, objectives and mathematical formulation of OPF problem including applicable constraints. The description of proposed algorithm is presented in Section-3. Section 4 presents various numerical results on a test system IEEE 30-bus and Algerian DZA

114-bus in order to show the capabilities of the developed algorithm. Finally, this paper is concluded with Section 5.

II. PROBLEM FORMULATION

The primary objective of OPF is to find the optimal settings of control-variables so that the specified objective-function is minimized while satisfying all constraints imposed (equality and inequality). Mathematically is formulated as follows:

$$\text{Minimize } F_{obj}(x,u) \tag{1}$$

$$\text{S.t. } g(x,u)\begin{cases} g(x,u)=0 \\ h(x,u)\le 0 \end{cases} \tag{2}$$

where $F_{obj}(x,u)$ is the objective function, $g(x,u)$ defines equality constraints, $h(x,u)$ inequality constraints. x and u are the vector of dependent variables and the vector of control variables, respectively. For obtaining the optimality and guarantee the feasibility of solutions, dependent variables also should be within the allowable limits, which play an essential role in the security of electric power system

A. OBJECTIVE FUNCTIONS

In this work, three objectives will be minimized, cost, power loss, and gas emissions of thermal units.

- *Thermal power only units:*

Fuel cost of thermal power units can be described as [17]:

$$C_{\mathrm{T0}}(P_{TG}) = \sum_{i=1}^{N_{TG}} a_i + b_i P_{TGi} + c_i P_{TGi}^2 \tag{3}$$

For more realistic pattern and precise modelling valve-point effect scheme is considered. Equation (3) is modified by adding an additional sine term to account for the valve effects in this manner:

$$C_{\mathrm{T}}(P_{TG}) = \sum_{i=1}^{N_{TG}} a_i + b_i P_{TGi} + c_i P_{TGi}^2 + \left| d_i \times \sin\left(e_i\left(P_{TG}^{\min} - P_{TG}\right)\right)\right| \tag{4}$$

where $a_i, b_i, c_i, d_i,$ and e_i are the cost coefficients of the $i^{-\mathrm{th}}$ thermal generators producing power output P_{TGi}, N_{TG} is the number of thermal generating and $P_{TG}^{\min}$ is the minimum of power of conventional thermal generator. The cost and emission gas coefficients for the conventional units used here are provided in [16].

Since wind and solar generators does not require any fuel like conventional thermal generators, cost-function evaluation of the wind and solar obey of some norms. The first norm is direct-cost for wind generator $Cost_{W,j}$ and solar generator $Cost_{S,k}$. Mathematically expressed as follows:

$$Cost_{W,j}\left(P_{WS,j}\right) = g_j P_{WS,j} \tag{5}$$

$$Cost_{S,k}\left(P_{SS,k}\right) = h_k P_{SS,k} \tag{6}$$

where g_j and h_k respectively, are the coefficient of direct-cost attached with j^{th} wind power plant and k^{th} solar power unit. $P_{WG,j}$ and $P_{SG,k}$ are the scheduled power from the same power plants (wind, solar).

Under the uncertainties, there are two possible scenarios: (1) if actual power-delivered by the wind farm or solar generator is less than the estimated-values, this scenario called as overestimation of power, herein the system operator needs to the spinning reserve to ensure uninterrupted supply to the consumers. The cost of committing the reserve production units to meet overestimated quantity is named as reserve-cost [1]. The reserve cost for wind and solar power units is written with following equations:

$$\begin{aligned} &Cost_{RW,j}\left(P_{WS,j} - P_{Av,j}\right) \\ &= K_{RW,j}\left(P_{WS,j} - P_{WAv,j}\right) \\ &= K_{RW,j}\int_0^{P_{WG,j}} \left(p_{WS,j} - P_{W,j}\right) f_W\left(P_{W,j}\right) dp_{W,j} \end{aligned} \tag{7}$$

$$\begin{aligned} &Cost_{RS,k}\left(P_{SS,k} - P_{SAv,k}\right) \\ &= K_{RS,k}\left(P_{SS,k} - P_{SAv,k}\right) \\ &= K_{RS,k} * f_S\left(P_{SAv,k} < P_{SS,k}\right) * \left[P_{SS,k} - E\left(P_{SAv,k} < P_{SS,k}\right)\right] \end{aligned} \tag{8}$$

where $K_{RW,j}$ denotes coefficient of reserve-cost pertaining to wind power plant, $P_{WA,j}$ is the actual available-power from the same plant. $f_W\left(P_{W,j}\right)$ is the Wind power PDF for j^{th} power plant where and more detail is given in [1]. $K_{RS,k}$ is the coefficient of reserve-cost for k^{th} Solar-Generator. $P_{SAv,k}$ is the actual available power from the same power-plant. $f_S\left(P_{SAv,k} < P_{SS,k}\right)$ is the probability of solar power-shortage occurrence than the scheduled power $(P_{SS,k})$, $f_s\left(P_{SAv,k} > P_{SS,k}\right)$ is the expectation of solar-power above $P_{SS,k}$.

Contrary of overestimation, the second scenario called the under estimation of wind/solar power plant. In this scenario the actual power produced is higher than the estimated one, yielding the surplus power. This situation requests introduce the penalty cost against each surplus amount of power, where expressed by the following equations.

$$\begin{aligned} &C_{PW,j}\left(P_{WAv,j} - P_{WS,j}\right) \\ &= K_{PW,j}\left(P_{WAv,j} - P_{WS,j}\right) \\ &= K_{PW,j}\int_{P_{WS,j}}^{P_{Wr,j}} \left(P_{W,j} - p_{WS,j}\right) f_W\left(P_{W,j}\right) dp_{W,j} \end{aligned} \tag{9}$$

$$\begin{aligned} &C_{PS,k}\left(P_{SA,k} - P_{SS,k}\right) \\ &= K_{PS,k}\left(P_{SAv,k} - P_{SS,k}\right) \\ &= K_{PS,k} * f_S\left(P_{SAv,k} > P_{SS,k}\right) * \left[E\left(P_{SAv,k} > P_{SS,k}\right) - P_{SS,k}\right] \end{aligned} \tag{10}$$

where $K_{PW,j}$ is the penalty cost coefficient for the $j^{-\mathrm{th}}$ wind power plant, $P_{Wr,j}$ is the rated output-power from the same wind-farm. $K_{PS,k}$ is the coefficient of penalty-cost for k^{th} solar PV plant. $f_S\left(P_{SAv,k} > P_{SS,k}\right)$ is the probability of solar power surplus i.e, actual power above the scheduled power $(P_{SS,k})$, $f_S\left(P_{SAv,k} > P_{SS,k}\right)$ is the expectation of solar power above $P_{ss,k}$. $E\left(P_{SAv,k} > P_{SS,k}\right)$.

It is important to indicate that the cost evaluation for wind generator and solar PV unit are depends on the wind Weibull probability-distribution-functions (PDF) and solar radiation by lognormal PDF respectively [23].

Case 1: In the first objective function, OPF is formulated with presence of RES, whereby all the cost-functions aforementioned are included. This objective minimizes the generation cost without including emission cost. Mathematically can be expressed as:

$$\begin{aligned} F_{Obj}^{1} &= C_T\left(P_{TG}\right) \\ &+ \sum_{j=1}^{N_{WG}} \left[\begin{array}{l} C_{W,j}\left(P_{WSs,j}\right) + C_{RW,j}\left(P_{WG,j} - P_{WAv,j}\right) \\ + C_{PW,j}\left(P_{WAv,j} - P_{WS,j}\right) \end{array} \right] \\ &+ \sum_{k=1}^{N_{SG}} \left[\begin{array}{l} C_{S,k}\left(P_{SS,k}\right) + C_{RS,k}\left(P_{SS,k} - P_{SAv,k}\right) \\ + C_{PS,k}\left(P_{SAv,k} - P_{SS,k}\right) \end{array} \right] \end{aligned} \tag{11}$$

where N_{WG} and N_{SG} denote the number of wind generators and PV solar in the grid.

Case 2: Emission gases and Carbon tax: Conventional thermal power generators emit harmful gases into the environment such as *SOX*, *NOX*, and CO_2, which pollute the atmosphere. To reduce emission of greenhouse gases, the carbon tax was imposed as penalty. This end can be achieved through minimization of generation and emission cost which can be expressed as follows:

Second objective function Minimize-

$$F_{Obj}^{2} = F_{Obj}^{1} + C_{tax} \times E \tag{12}$$

$$\begin{aligned} E = \sum_{i=1}^{N_{TG}} \Big[&\left(\alpha_i + \beta_i P_{TGi} + \gamma_i P_{TGi}^{2}\right) \\ &\times 0.01 + \omega_i \exp\left(\mu_i P_{TGi}\right) \Big] \end{aligned} \tag{13}$$

where α_i, β_i, $\gamma_i\omega_i$, μ_i are the emission-coefficients corresponding to the i^{-th} generator and C_{tax} is the carbon tax, which is equal to 20 ($/h).

B. SYSTEM CONSTRAINTS

- *Equality-constraints*: are the power flow equations which are given below:

$$\begin{cases} P_{Gi} - P_{di} - \sum_{j=1}^{NB} |V_i| \times \left|V_j\right| \times \left|Y_{ij}\right| \\ \quad \times \cos \times \left(\theta_{ij} - \delta_i + \delta_j\right) = 0 \\ Q_{Gi} - Q_{di} - \sum_{j=1}^{NB} |V_i| \times \left|V_j\right| \times \left|Y_{ij}\right| \\ \quad \times \sin \times \left(\theta_{ij} - \delta_i + \delta_j\right) = 0 \end{cases} \tag{14}$$

- *Inequality constraints: represent the limits applied on the following variables*

$$P_{TGi}^{\min} \le P_{TGi} \le P_{TGi}^{\max}, \quad i = 1, 2. \ldots . N_{TG} \tag{15}$$

$$P_{Wsj}^{\min} \le P_{\mathrm{W}sj} \le P_{Wsj}^{\max}, \quad j = 1, 2. \ldots . N_{WG} \tag{16}$$

$$P_{SG,k}^{\min} \le P_{SG,k} \le P_{SG,k}^{\max} \quad k = 1, 2. \ldots . N_{SG} \tag{17}$$

$$Q_{TGi}^{\min} \le Q_{TGi} \le Q_{TGi}^{\max}, \tag{18}$$

$$Q_{Wsj}^{\min} \le Q_{Wsj} \le Q_{Wsj}^{\max}, \quad i = 1, 2 \ldots . . N \tag{19}$$

$$Q_{SG,k}^{\min} \le Q_{SG,k} \le Q_{SG,k}^{\max} \quad k \in N_{SG} \tag{20}$$

$$Q_{Ci}^{\min} \le Q_{Ci} \le Q_{Ci}^{\max} \quad i \in N_C \tag{21}$$

$$V_{Gi}^{\min} \le V_{Gi} \le V_{Gi}^{\max}, \tag{22}$$

$$V_{Li}^{\min} \le V_{Li} \le V_{Li}^{\max} \quad i \in NL \tag{23}$$

- Security constraints

$$T_k^{\min} \le T_k \le T_k^{\max} k \in NT \tag{24}$$

$$S_i \le S_i^{\max} i \in NTL \tag{25}$$

Eqs, (15) − (17) are the active power limits of conventional power-plants, wind and solar power generators, respectively. Eqs, (18) − (21) are the reactive power capabilities of conventional power-plants, wind-/ solar generators and shunt reactive power sources. Eq, (22) shows the constraints applied at the generators busbar, whereas Eq, (23) represents the voltage limits constraining load-buses, *NL* being the number of load-buses. Security-Constraints of: tap changing transformer and line capacity are given by Eqs, (24) (25), respectively. *NTL* is the number of lines in the electric grid.

In handling constraints, one of the first widely adopted approaches employed is static-penalty function method which is commonly based on trial and error. However, improper selection of penalty-coefficients may sometimes lead to violation of system constraints. To this purpose, constraint handling technique, superiority of feasible solutions (SF) is employed for guaranteeing the feasibility of solutions.

- *Superiority of feasible solutions (SF)*

This approach was first proposed by *Powell* and *Sklonick* in 1993 to deal infeasible solutions, afterwards Deb in [24] propose similar technique which transform the equality constraints to inequality constraints with aid of a tolerance factor epsilon ε by using Eq. (26). Mathematically described as follows:

$$\text{fitness}\,(x) = \begin{cases} f\left(\overrightarrow{x}\right) \text{ if } h_i\left(\overrightarrow{x}\right) \ge 0 \\ \qquad \forall i = 1, 2, \ldots . . , N \\ f_{worst} + \sum_{i=1}^{N} h_i\left(x\right) \\ \qquad otherwise, \end{cases} \tag{26}$$

$$\left|g_i\left(x\right)\right| - \varepsilon \le 0 \tag{27}$$

where f_{worst} is the objective function value of the worst feasible solution in the population and if there are no feasible solutions in the population, then f_{worst} is set to zero. ε is a tolerance parameter for the equality-constraints. Other mathematical expression of SF method is presented as follows:

$$T_i\left(x\right) = \begin{cases} \max\left\{h_i\left(x\right), 0\right\} & i = 1, \ldots . , N \\ \max\left\{\left|g_i\left(x\right)\right| - \varepsilon,\ 0\right\} & i = N+1, \ldots . , M \end{cases} \tag{28}$$

Therefore, the aim is to minimize a desired objective function $F_i(X)$ so that the optimal solution subjected to all inequality constraints $T_i(X)$. The overall constraint violation for an infeasible individual is a weighted mean for all the constraints, which is presented as:

$$v_i(x) = \frac{\sum_{i=1}^{N} w_i [T_i(x)]}{\sum_{i=1}^{N} w_i} \tag{29}$$

when we compare two solutions X_i and X_j, X_i is said superior to X_j under the following conditions:

1) A feasible point is preferred over an infeasible one
2) Between two feasible solutions, solution having a smaller objective-value in a minimization case (greater objective value in case of maximization) is preferred.
3) Between two infeasible solutions, the one that has a smaller constraint violation is chosen.

More detail on different constraint-handling techniques for meta-heuristic optimization can be found in [25], [26].

C. STOCHASTIC WIND/SOLAR AND UNCERTAINTY MODELS

Since wind speed is a random variable, its distribution is obtained by Weibull Probability Density Function (PDF) with shape factor (k) and scale factor (c). Mathematically given by:

$$f_v(S) = \left(\frac{k}{c}\right)\left(\frac{S}{c}\right)^{(k-1)} \times \exp - \left(\frac{S}{c}\right)^{k} \quad for\ 0 < S < \infty \tag{30}$$

- *Wind power model*
  The output wind power from a wind turbine is a function of wind speed, expressed by the following equation: [16]

$$P_w(\upsilon) = \begin{cases} 0, & \text{for } \nu \langle \nu_{in} \text{ and } \nu \rangle \nu_{out} \\ P_{wr}\left(\dfrac{\nu - \nu_{in}}{\nu_r - \nu_{in}}\right) & \text{for } \nu_{in} \le \nu \le \nu_r \\ P_{wr} & \text{for } \nu_r \le \nu \le \nu_{out} \end{cases} \tag{31}$$

  where ν_{in}, ν_r and ν_{out} are respectively the turbine cut-in, rated and cut-out wind speeds. P_{wr} defines the rated output power of the wind turbine.
- *Wind power probability for different wind speeds*
  From eq. 32, we can note that if ν is less than ν_{in} and above ν_{out}, the power output is zero. Also, the wind turbine produces P_{wr} for the condition $\nu_r \le \nu \le \nu_{out}$. For these discrete zones, the probabilities can be written by the following equations:[27]

$$f_w(P_w)\{P_w = 0\} = 1 - \exp\left[-\left(\frac{\nu_{in}}{\alpha}\right)^{\beta}\right] + \exp\left[-\left(\frac{\nu_{out}}{\alpha}\right)^{\beta}\right] \tag{32}$$

$$f_w(p_w)\{p_w = p_{wr}\} = 1 - \exp\left[-\left(\frac{\nu_r}{\alpha}\right)^{\beta}\right] + \exp\left[-\left(\frac{\nu_{out}}{\alpha}\right)^{\beta}\right] \tag{33}$$

Unlike to the discrete zones, the output wind power is continuous for the condition $\nu_{in} \le \nu \le \nu_r$, Hence the probability for this region is described as follows: [27]

$$f_w(p_w) = \frac{\beta(\nu_r - \nu_{in})}{\alpha^{\beta} * P_{wr}}\left[\nu_{in} + \frac{P_w}{P_{wr}}(\nu_r - \nu_{in})\right]^{\beta-1} \times \exp\left[-\left(\frac{\nu_{in} + \frac{P_w}{P_{wr}}(\nu_r - \nu_{in})}{\alpha}\right)^{\beta}\right] \tag{34}$$

Also, the solar irradiance to energy conversion for the PV plant also can be given by

$$P_s(G) = \begin{cases} P_{sr}\left(\dfrac{G^2}{G_{std} R_c}\right) & \text{for } 0 \le G \le R_c \\ P_{sr}\left(\dfrac{G^2}{G_{std}}\right) & \text{for } G \ge R_c \end{cases} \tag{35}$$

where G_{std}, is the solar irradiance in standard environment, R_c is a certain irradiance point, P_{sr} is the rated output of the PV power plant. Further details about uncertainty model of RES can be found in Ref [1].

III. SMA-BASED PROPOSED METHOD

Slime Mold Algorithm is a novel stochastic optimization technique proposed by Li *et al.* in 2020 [22], that has tried to mimics the behavior of *Physarum polycephalum* and the bio-oscillation mode of the slime in nature. SMA used the weights to simulate the negative and positive feedback produced by slime mold during foraging-process, forming three kinds of morphotype. The latter is regarded as a new idea involves creating a differentiation in search-space for obtaining new possible solutions. One of the most interesting characteristics of slim mould is the unique pattern, allowing to SM custom several foodstuff sources simultaneously, forming a venous network joining them. This pattern allows exploring different regions of search-space and avoids falling into local optima. Based on the quality food-stuff, slim mould can well-being dynamically adapt or adjust their search schemes efficiently. When the quality of food sources is positive (high-quality), the slim mould utilizes the region-limited search-technique, herein slim mould focuses only on the achieved food sources. Otherwise, in case of quality of food sources that have been found is negative (low- quality), they abandon the food source in order to explore new ones in the area. According of the negative, positive feedback responses, slime mould can develop the optimum food-path to tie food in a relatively more best way. The mathematical model of some mechanisms and characteristics of the slime mould will be illustrated in the subsequent sections.

FIGURE 1. Foraging morphology of SM.

A. MATHEMATICAL MODELING OF THE SLIME MOULD ALGORITHM

1) APPROACH-FOOD

SM can easily reach food through the odour in the air. This behavior of contraction is modeled mathematically Eq.(30)

$$\overrightarrow{X\,(t+1)} = \begin{cases} \overrightarrow{X_b\,(t)} + \overrightarrow{vb}.\left(\overrightarrow{W}.\overrightarrow{X_A\,(t)} - \overrightarrow{X_B\,(t)}\right), & r < p \\ \overrightarrow{vc}.\overrightarrow{X\,(t)}, & r \geq p \end{cases} \tag{36}$$

where $\overrightarrow{vb}$ is a parameter within range [−a, a], $\overrightarrow{vc}$ decreases linearly from 1 to 0. t represents the current iteration. $\overrightarrow{X_b}$ indicates the individual position associated with highest odour-concentration currently found. $\overrightarrow{X}$ represents the position of SM, $\overrightarrow{X_A}$ and $\overrightarrow{X_B}$ are two randomly generated individuals from the population. W is the weight of slime mould. The p formula expressed by Eq. 38

$$p = tngh\,|S\,(i) - DF| \tag{37}$$

where $S\,(i)$ is the fitness value of $\overrightarrow{X}$, whereas DF is the best fitness obtained in all iterations. $\overrightarrow{vb}$ is defined as follows: $vb = [-a, a]$

$$a = arctanh\left(-\left(\frac{iter}{max - iter}\right) + 1\right) \tag{38}$$

The formula of W in Eq. (1) can be given by

$$\overrightarrow{W\,(SmellIndex)} = \begin{cases} 1 + r.log\left(\dfrac{bF - S\,(i)}{bF - wF} + 1\right), & Condition \\ 1 - r.log\left(\dfrac{bF - S\,(i)}{bF - wF} + 1\right), & others \end{cases} \tag{39}$$

Eq. 34 simulates the negative and positive feedback created between the concentration foods explored with the vein width of the SM.

$$SmellIndex = sort\,(S) \tag{40}$$

where r is a randomly generated number with a range of [0, 1] and bF represents the optimum fitness-value obtained in the current-iteration. The worst fitness-value realized in the iterative process currently is wF. $SmellIndex$ defines the sequence of fitness-values sorted. log is introduced to ease the change-rate of numerical value, in which the contraction frequency value does not change significantly

2) WRAP-FOOD

A slime mould will update its location with the following formula:

$$X^* = \begin{cases} rand.\,(ub - lb) + lb, & rand < z \\ \overrightarrow{X_b\,(t)} + \overrightarrow{vb}.\left(W.\overrightarrow{X_A\,(t)} - \overrightarrow{X_B\,(t)}\right) & \\ \overrightarrow{vc}.\overrightarrow{X\,(t)}, & r \geq p, \\ r < p & \end{cases} \tag{41}$$

where ub and lb are the upper and lower bounds of search-space, respectively

3) GRABBLE-FOOD

The success of SM mainly depends on their oscillation parameters vb and vb, were used to introduce stochastic nature in the model, helping to guide individuals towards food position having high concentration. Detailed characteristics about slime mould algorithm is given in [22]. SMA is like other meta-heuristic techniques start the process of optimization by distributing individuals in the search-space as first solutions. Each individual in a population represents a possible solution of the optimization problem, and then all generated solutions have been evaluated by selected objective-function and select the minimal value with minimization and maximum value in case of maximization.

Afterwards, at each iteration the individuals update their coordinates according to some equations movement of slime mould in nature along with some parameters.

In the next step, the updating process is repeated till a terminal criterion is satisfied. Last step, the optimal-solution that corresponds to the best-individual achieved so far is memorized. Table 1 describes the steps of the proposed SMA in solving OPF problem considering WT and PV generation. with SF constrain approach. The flowchart of proposed algorithm is presented in **Fig 2**.

IV. NUMERICAL RESULTS AND DISCUSSION

To validate the potential and feasibility of the proposed SMA in solving stochastic OPF problems incorporating wind power generators and solar photovoltaic, SM algorithm was examined on the modified IEEE 30-bus test system and Algerian electricity grid DZA 114-bus under different objective functions. The modification is to insert two wind generators at buses #5 and #11along with one solar generator at bus #13. All data ca be retrieved in [23] and Zimmerman *et al.* [28]. All algorithms have been coded and solved under MATLAB R2014a platform and run on an Intel®Core™i5-4300U 2.50 GHz 4.00 GB RAM personal computer. The population size is selected using empirical tests by running the SMA several times with different population sizes like 20, 40, 60 and 80. The test results are

TABLE 1. SMA for stochastic optimal power flow (OPF) prpblem.

Step 1	• Read data of test system and SMA-SF input
	• Read input data of test system configuration: Bus-data, Line-data, transformers data, and generation units-data.
	• Dimension of the problem, dim (dim =12 for IEEE 30-bus, 30 for DZA114-bus)
	• Number of population, N_P (N_P = 30 for IEEE 30-bus and 60 for DZA 114-bus, Selected)
	• Stopping criteria is the Max-number of iterations
	• Minimum and Maximum value of control (decision) variables, in vector like $X_{\min}$ and $X_{\max}$ $X_{\min}=\left[X^{1}_{\min},X^{2}_{\min},.....,X^{\dim}_{\min}\right]$ and $X_{\max}=\left[X^{1}_{\max},X^{2}_{\max},.....,X^{\dim}_{\max}\right]$
Step 2	• Specify the desired objective function to be optimized (F^{1}_{Obj} , F^{2}_{Obj} , or F^{3}_{Obj})
Step 3	• Calculate the forecasted-output power of wind turbine and PV units.
Step 4	• Generate initial population of size N_P individuals uniform spreading in the range [$X_{\min}$, $X_{\max}$]
Step 5	• Run power-flow for each updated individual in the population and calculate the fitness of all individual. Then, evaluate constraint function and constraint violation using Equations. (27) – (30).
Step 6	• Apply the SMA operators and equations of update to create a new population of individuals' (i.e., obtaining Improved solutions of the problem).
Step 7	• In selection phase, individuals for next population are replaced with new individuals if give better value of objective func according to rules of SF method. After each updating process, the new individual is considered better if it yields negligit constraint violation or zero constraint violation than the respective old population individual. Otherwise, previous indivi is retained.
Step 8	• Repeat steps **5-7** until the stopping criteria is reached, i.e., until max-iteration achieved
Step 9	• Report the optimal results that corresponds with the best pathfinder and its fitness value (objective-function value)

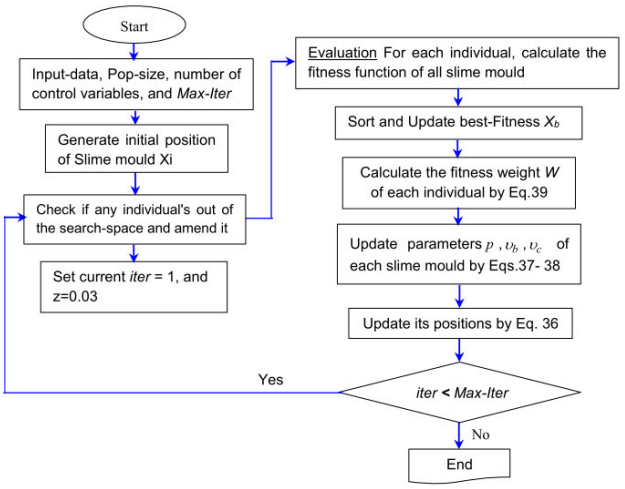

FIGURE 2. Flowchart of SMA.

not reported herein, we therefore, indicate only the population size which resulted in achieving best outcomes. To this end, in all simulation cases, number of population size is specified as 30 individuals for IEEE 30-bus, 60 for DZA 114-bus and maximum number of iterations is fixed 300 for IEEE 30-bus and 400 for practical power system. For the purpose of a fair comparison, all control variables of test systems were considered as continuous. Table 2 provides PDF parameters of wind power and solar PV plants.Table 3 reports description of all test-systems characteristics used in this article.

A. RESULTS OF MODIFIED IEEE 30-BUS TEST SYSTEM

To show the efficiency of the SMA, the deterministic OPF cases for the modified system configuration, i.e., without WT generators and PV units are considered. Four cases are studied herein, with the objective functions mentioned in section above, namely: Case 1– minimization of basic fuel cost; Case 2 – optimized cost against reserve-cost; Case 3 – minimization of total generation-cost with carbon-emission tax; Case 4 – optimized cost against penalty-cost. The optimal results obtained for each examined case are presented in Table 4.

1) CASE 1– MINIMIZATION OF TOTAL GENERATION-COST

In this case, the objective-function is minimization of the total cost of generation. Obtained findings by using proposed algorithm SMA are based on the Weibull PDF parameters. Figures 3-5 represent Weibull fitting and wind distribution obtained from the simulation of 8000 Monte Carlo scenarios, while the stochastic power-output of solar photovoltaic unit is illustrated by Fig 6.

Optimal locations of the wind farm and PV power generation depend on several factors such as wind speed and solar radiation, respectively [29].

In this paper, the locations of wind and PV units are selected as in [30] for IEEE 30-bus test system with the aim of comparing the obtained results with those mentioned in [30]

TABLE 2. PDF parameters of WG and SG system IEEE 30-Bus.

Wind-power generating units				
Position of Windfarm	No of turbines	Rated power, P_{wr} (MW)	Weibull PDF parameters	Weibull mean, M_{wbl}
Bus # 5	25	75	c = 9 k = 2	v = 7.976 m/s
Bus #11	20	60	c = 10 k = 2	v = 8.862 m/s
Photovoltaic power plant				
Position of Solar system	Rated power, P_{rv} (MW)		Lognormal PDF parameters	Lognormal mean
Bus #13	50		μ= 6, r = 0.6	G = 483 W/m^2

TABLE 3. Test-systems characteristics description utilized.

Parameter	IEEE 30-bus	DZA 114-bus
Buses, N_B	30	114
Generators, N_G	6	15
Transformers, N_T	4	16
Shunts, N_Q	9	7
Branches, N_E	41	175
Control variables	12	46
Base case for P_{Loss}, p.u.	5.880	67.447
Base case for VD, p.u.	1.4942	3.82
Algorithms parameter setting		
Dimension of optimization problem (dim)	12	30
Population size	30	60
Max Iteration	300	400

and from company of electricity SONELGAZ for Algerian power system.

As shown, from obtained findings the SMA, given in Table 4 is achieved the minimum value of generation cost compared with other optimizers. The optimal generation cost achieved by SMA is 781.078 MW, while for other optimization techniques, PSO (784.3400 $/h), TLBO (782.6767 $/h), SHADE-SF (782.50$/h), jellyfish (781.6387 $/h), artificial ecosystem optimizer (781.5219 $/h), and hunger games search (781.86 $/h) as well as vs. a recently optimization technique which introduced October 1, 2021 entitled, orca predation algorithm (782.0760 $/h) and gorilla troops optimizer GTO (781.26 $/h). It is worth to note that PWG1 and PWG2 indicate the scheduled powers from wind generators #WG1 and #WG2, respectively. The emission rate is calculated by using the optimal scheduled power of thermal generators, where reserve is assumed an alternate source that does not add to the emission.

Based on the results obtained in the literature regarding solution of classical OPF problem and the results given in

Table 4, it can state that with insertion of renewable energy sources, the total generation-cost decreased from 800.00 $/h as a reference cost to 781.07 ($/h), i.e., around 18.9 $/h. More precisely, if every hour can save the cost of 18.9 $, and the operating time per-year is supposed as 7500 h, then operating time from the propose optimizer SMA can save 141975 Dollars in total every year. Consequently, the

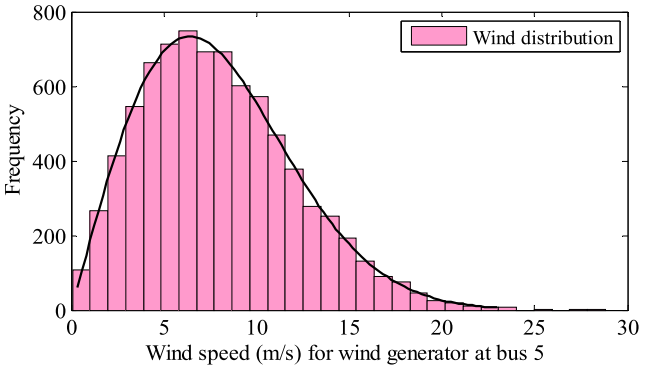

FIGURE 3. Wind speed distribution for wind-power Generator#1 at bus 5 (c = 9, k = 2).

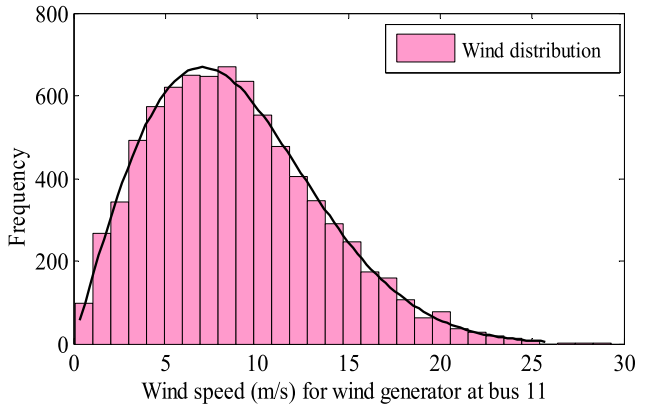

FIGURE 4. Wind speed distribution for wind-power Generator#1 at bus 11 (c = 10, k = 2).

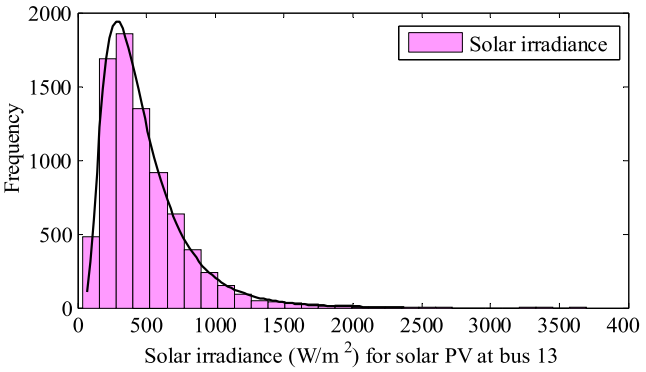

FIGURE 5. Distribution of solar irradiance or solar PV generator at bus #13 (μ = 6, σ = 0.6).

insertion of wind generators and solar power plant significantly contributes on the reduction on total generation cost compared with the original system configuration (i.e., without RES). The comparison and statistical- results of SMA with other algorithms are listed in Table 5. Fig. 7, illustrates a comparison between the convergence of SMA and other applied algorithms.

2) CASE 2– MINIMIZATION OF TOTAL GENERATION-COST WITH CARBON-EMISSION TAX

In this case, the quadratic total cost of generation and emission functions in (13) were minimized considering the

TABLE 4. Optimal results comparison for different algorithms for IEEE 30-bus, Case 1.

Variables	Min	Max	PSO [23]	TLBO [32]	SHADE-SF [1]	JS [30]	OPA	AEO	HGS	GTO	SMA
P_{TG1}	50	140	134.907	134.843	134.908	134. 905	134.91	134. 908	134.907	134.907	134.91
P_{TG2}	20	80	28.037	29.0639	28.564	29.0226	27.0785	27.7985	28.8317	28.1779	29.4961
$P_{WG}1$	0	75	43.744	44.045	43.774	43.9696	43.0040	42.9166	42.8527	43.2909	42.2527
P_{TG3}	10	35	10.000	10.0606	10	10.0006	10.0003	10.0037	10.0000	10.0000	10.0034
P_{WG2}	0	60	37.193	36.6258	36.949	37.0193	36.4374	35.9806	35.3547	36.5917	37.1432
P_{SG1}	0	50	35.303	34.5823	34.976	34.2532	37.7603	37.9418	37.2989	36.1438	35.3402
V_1	0.95	1.1	1.0815	1.0756	1.072	1.07725	1.0724	1.075	1.0757	1.0725	1.0726
V_2	0.95	1.1	0.9500	1.0587	1.057	1.05698	1.0568	1.058	1.0606	1.0578	1.0590
V_5	0.95	1.1	1.1000	1.0411	1.035	1.03507	1.0346	1.035	1.0385	1.0374	1.0349
V_8	0.95	1.1	1.1000	1.0353	1.04	1.03705	1.0392	1.038	1.0422	1.0395	1.0396
V_{11}	0.95	1.1	1.1	1.0874	1.1	1.0983	1.0981	1.100	1.1000	1.1000	1.1000
V_{13}	0.95	1.1	1.0626	1.0359	1.055	1.04571	1.0566	1.074	1.0582	1.0548	1.0511
Q_{TG1}	-20	150	15.6792	4.51	-1.903	-0.68357	-0.89148	5.97209	1.97011	-2.64234	-4.56703
Q_{TG2}	-20	60	- 20	12.0447	13.261	11.00115	12.33114	15.9173	19.89941	12.51218	17.69608
Q_{WG4}	-30	35	35.00	29.9474	23.181	22.6673	23.18025	33.7725	26.51019	4.65643	1.98405
Q_{TG3}	-15	40	40.00	30.7341	35.101	40.0	134.91	25.7527	39.23979	32.04730	32.68252
Q_{WG5}	-25	30	27.85	27.9642	30	30	29.98468	29.8473	30.000	29.70313	29.90060
Q_{SG6}	-20	25	17.73	11.8604	17.346	14.0246	18.13988	24.4921	17.94308	16.09073	14.70039
F_{Cost} ($/h)	782.242	782.359	781.90	782.6767	782.503	781.6387	782.0760	781.3979	781.86	781.2626	781.0786
VD	NR	NR	NR	NR	NR	0.4421	0.46629	0.5279	0.48809	0.4838	0.47015
P_L	NR	NR	NR	NR	NR	5.7738	5.7882	5.7950	5.8460	5.7117	5.7502
T (s)	NR	NR	NR	NR	NR	NR	1221	429.7	287.8	357.9	286.7

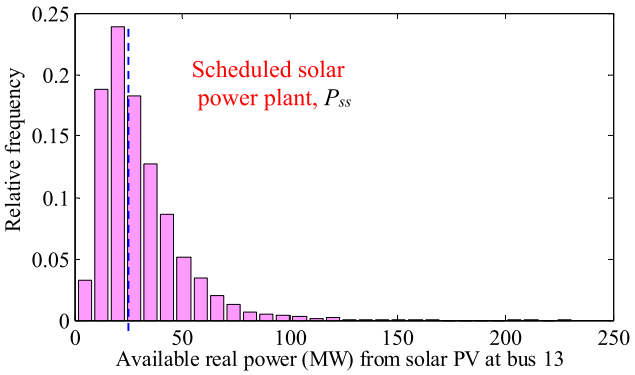

FIGURE 6. Real power distribution (MW) of solar PV at bus 13.

TABLE 5. Statistical results of different optimizers for Case 1.

Algorithms	Min ($/h)	Max ($/h)	Mean ($/h)	Std
GOA [23]	785.7109	823.4731	804.016837	9.52e + 00
BWOA [23]	784.8148	795.4683	788.247149	5.83e + 00
GWO [23]	781.6645	783.3359	783.041218	2.75e - 01
ALO [23]	781.6562	791.9234	784.325274	2.49e + 00
PSO [23]	781.9047	794.4220	784.904776	2.52e + 00
GSA [23]	782.2237	794.8995	785.860254	2.43e + 00
MFO [23]	781.6928	783.9304	782.49197	4.77e - 01
BMO [23]	781.6519	783.5283	781.81867	3.44e - 01
AEO	781.3979	782.8744	781.8199	3.095e - 01
HGS	781.86	782.9445	782.4106	3.649e - 01
GTO	781.2626	782.7022	782.082	3.77e - 01
SMA	781.07	782.990	781.9726	4.53e - 01

carbon tax (Ct) imposed on the thermal power plants. Herein, the carbon-tax value is equal to 20 $/ton [1]. It is obvious that with existence of the Carbon-Tax the penetration level from RES is raised, and this can be visualised within simulation results. The ratio of penetration of RES in the scheduled of optimum generation is based on the volume of emission rate with the imposed carbon-tax value. Main objective here is to schedule more power among the renewable energy so that the volume of emission is kept at minimum level.

3) CASE 3 – OPTIMIZED COST AGAINST RESERVE-COST

In third case, all parameters are retained the same as in first case except reserve-cost-coefficients. The coefficients of wind generators and solar photovoltaic unit are varied by a discrete-step of 1 starting from 4 to 6, i.e., = 4, (case3-a), = 5, (case3-b) = 6, (case3-c). The penalty-cost-coefficients for all intermittent sources are remain the same as the first case. The optimal power scheduled of generators is presented by bar graph in Fig.8 and compared with those found for the base case (case 1). For clarification purpose, Case 3-a describes case when reserve coefficient $K_r = 4$, case 3-b represents for $K_r = 5$, and case 3-c represents $K_r = 6$. In this case study, when the coefficient of reserve cost increases, the

TABLE 6. Optimal results of case 2 for modified IEEE 30-bus test system.

Variables	SHADE-SF [23]	MFO [23]	BMO [23]	JS [30]	OPA	HGS	GTO	AEO	SMA
P_{TG1}	123.020	123.637	123.127	123.572	123.914	123.3155	123.3721	123.394	123.6670
P_{TG2}	33.047	33.2996	31.947	33.1626	34.5124	32.6554	32.7853	32.6311	33.5199
P_{WG1}	46.021	46.1099	45.402	46.0806	46.6065	45.7569	45.8351	45.8296	46.2945
P_{TG3}	10.00	10.0000	10.000	10.00	10.00	10.00	10.00	10.000	10.000
P_{WG2}	38.748	38.8443	38.270	38.8011	39.1231	38.5231	38.5999	38.5619	39.2413
P_{SG1}	37.336	36.7199	39.865	37.0628	34.5273	38.4482	38.0833	38.2888	35.9774
V_1	1.071	1.0782	1.0777	1.07066	1.0715	1.0723	1.0702	1.0732	1.0731
V_2	1.057	1.0645	1.0640	1.05715	1.0583	1.0591	1.0569	1.0588	1.0589
V_5	1.036	1.0432	1.0426	1.03604	1.0364	1.0384	1.0357	1.0371	1.0378
V_8	1.04	1.0473	1.0471	1.04038	1.0399	1.0427	1.0403	1.0415	1.0414
V_{11}	1.099	1.1000	1.1000	1.0983	1.0975	1.1000	1.0985	1.0983	1.0980
V_{13}	1.056	1.0591	1.0602	1.05575	1.0521	1.0627	1.0580	1.0573	1.0581
Q_{TG1}	-2.678	- 1.738	- 1.8489	-2.6666	-2.75418	-0.0912	-3.24025	2.9900	2.4424
Q_{TG2}	12.319	12.565	12.4064	12.3540	14.63630	18.527	12.55509	17.7547	17.9378
Q_{WG4}	35.27	22.889	22.9177	35.2538	22.6387	26.0632	22.83972	25.5261	25.9879
Q_{TG3}	22.964	35.847	35.6862	22.9990	34.70553	39.9714	34.9987	39.8429	39.5619
Q_{WG5}	30	28.500	28.5058	30.00	29.98716	30.00	30.00	29.9998	29.8480
Q_{SG6}	17.779	16.659	17.0942	17.7114	16.44832	19.737	18.50504	18.1606	18.5039
F_{Cost} ($/h)	810.346	811.422	810.7982	810.120	811.121	811.0344	810.4412	810.7258	**810.3875**
Emission	0.891	NA	NA	0.8937	0.9114	0.8807	0.88361	0.8847	**0.8986**
VD (p.u.)	0.469	NA	NA	0.4688	0.4592	0.5042	0.47525	0.4731	0.4760

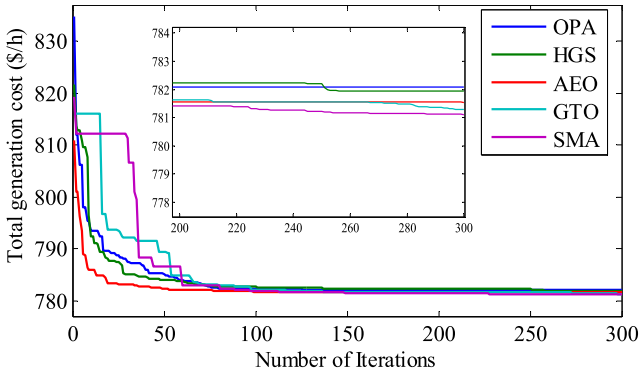

FIGURE 7. Convergence curves of different optimization techniques for case1.

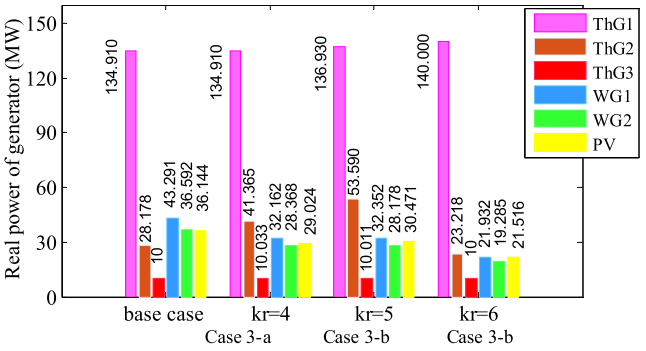

FIGURE 8. Variation of optimal scheduled real-power against reserve cost coefficient.

contribution of wind and solar generators reduced gradually, resulting in a shortage of scheduled power. So, an amount of spinning reserve is urgently needed in order to fill this shortage. This shortage in power automatically compensated by thermal generators which result in increasing the cost of thermal power generators due to the increase of the output power illustrated in Figure 7. In summary, total generation cost raises with the increase in the reserve-cost coefficient.

B. CASE 4 – OPTIMIZED COST AGAINST PENALTY-COST

Unlike to the past case, in the fourth case, all parameters of reserve cost are keeping as in first case excluding penalty cost-coefficients. Then coefficients of penalty-cost for all wind generators and photovoltaic power plant are raised from 4 to 6 by the following order, i.e., = 4 (case 4-a), = 5 (case 4-b), = 6 (case 4-a). The optimal power scheduled of six-generators is represented by bar-graph in Figure 9 and compared with those found for the case 1 at the same figure.

When penalty cost coefficient raises, scheduled amount of renewable energy generators increases too, leading to decrease the output of thermal generating units with a not uniform manner, Figure 9. This is judged on the basis of the economic dispatch between three thermal generators, and it is observed that considerable part of power is dispatched on the generator which having the lower production cost. On the other hand, the scheduled output for all renewable energy sources also seems not to uniform, which can be interpreted by the highly nonlinear relation between PDF and reserve / penalty cost of both solar and wind generators. It is also seen that the thermal generators cost Th_{Gx} is constant and a steady rise in total cost is observed

TABLE 7. Solution of optimal power flow case 1 for DZA 114-bus system.

Control variables	MIN	MAX	Base case	OPA	HGS	GTO	AEO	SMA
P_{TG4}	135	1350	450.8996	413.2818	404.4582	400.3014	416.6021	413.2914
P_{TG5}	135	1350	451.3313	428.551	446.8119	416.6813	420.5881	411.7038
P_{TG11}	10	100	99.9974	99.2632	100	100	99.9744	100
P_{TG15}	30	300	193.0450	168.5094	170.2331	175.3476	176.8195	177.3124
P_{TG17}	135	1350	444.4532	390.1661	387.1318	402.5487	396.6578	392.3503
P_{TG19}	34.5	345	196.1699	171.5505	164.9564	190.5869	165.1977	169.5086
P_{TG22}	34.5	345	190.8192	160.7105	164.1984	148.5535	163.3672	165.9908
P_{WG52}	0	345	193.1113	344.9866	345	345	344.9751	344.9997
P_{TG80}	34.5	345	193.9922	172.6886	157.7876	158.4923	160.3047	158.0744
P_{WG83}	0	300	186.6383	299.9742	300	300	299.9913	299.9990
P_{TG98}	30	300	187.5137	153.098	157.9963	161.5886	160.0757	162.2803
P_{TG100}	60	600	600	598.5746	600	600	599.4559	600
P_{TG101}	20	200	200	199.9995	200	200	199.9034	200
P_{TG109}	0	100	99.9996	99.7473	100	100	99.7655	100
P_{TG111}	10	100	100	99.9309	100	100	99.8781	99.9982
V_{G4}	0.9	1.1	1.0804	1.0968	1.0116	1.0858	1.0212	1.0979
V_{G5}	0.9	1.1	1.0737	1.0876	1.0043	1.0785	1.0136	1.0909
V_{G11}	0.9	1.1	1.0722	1.0947	1.0152	1.0810	1.0029	1.100
V_{G15}	0.9	1.1	1.0825	1.0986	1.0150	1.0882	1.0243	1.0989
V_{G17}	0.9	1.1	1.0770	1.0904	1.0260	1.0847	1.0500	1.0879
V_{G19}	0.9	1.1	1.0779	1.0585	1.0290	0.9895	0.9674	1.0629
V_{G22}	0.9	1.1	1.0839	1.0601	1.0693	1.0117	0.9724	1.0783
V_{G52}	0.9	1.1	1.0566	1.0434	1.100	1.0679	1.0239	1.1000
V_{G80}	0.9	1.1	1.0589	1.0518	1.0565	1.0518	1.0258	1.0448
V_{G83}	0.9	1.1	1.0991	1.0975	1.100	1.0956	1.0663	1.0813
V_{G98}	0.9	1.1	1.0868	1.0909	1.0754	1.0868	1.0626	1.0897
V_{G100}	0.9	1.1	1.0994	1.0999	1.100	1.0958	1.0851	1.1000
V_{G101}	0.9	1.1	1.0834	1.0973	1.0749	1.100	1.0726	1.0989
V_{G109}	0.9	1.1	0.9898	1.0898	1.0683	1.100	1.0571	1.0991
V_{G111}	0.9	1.1	1.1000	1.0597	1.0461	1.0259	1.0308	1.0585
Q_{TG4}	-20	400	298.3307	349.0682	286.1607	327.1684	314.5466	313.9243
Q_{TG5}	-20	200	199.3643	168.2862	199.6320	194.7538	198.9920	199.0592
Q_{TG11}	-50	100	81.10112	86.33829	98.69637	79.75229	62.2977	91.3217
Q_{TG15}	0	100	53.32891	60.94236	64.01384	58.76674	62.9398	53.1718
Q_{TG17}	0	400	342.62931	384.7696	304.7518	350.3737	390.6332	359.4238
Q_{TG19}	0	60	59.61001	58.40164	57.88848	48.95479	41.5081	52.4364
Q_{TG22}	0	50	49.33451	45.2415	48.42180	49.06288	49.3054	42.9558
Q_{WG52}	0	50	49.70127	23.09849	46.71148	44.14135	49.1808	40.0930
Q_{TG80}	0	60	59.98839	59.7900	59.78096	54.25570	56.6036	59.3190
Q_{WG83}	-50	200	191.14717	170.939	182.0681	174.2384	135.3155	120.3458
Q_{TG98}	0	50	47.66524	48.7959	47.91710	49.59778	29.5177	49.7116
Q_{TG100}	0	270	130.8002	118.6411	197.2178	116.5047	221.6016	160.7439
Q_{TG101}	-50	200	138.11934	151.9662	155.4020	175.5691	172.4061	155.0638
Q_{SG109}	-50	100	-2.22395	27.20327	34.71469	30.70667	29.1999	28.7393
Q_{TG111}	-50	155	90.0308	74.29622	75.90868	64.92301	75.6699	74.7460
F_{Cost} ($/h)			**18942.2799**	16811.17	16794.44	16795.02	16767.82	**16693.11**
VD (p.u)			4.3034	3.428	3.7598	3.8629	3.01914	5.3316
Ploss (MW)			60.9708	74.0320	71.5737	72.1003	76.5565	**68.5089**
$\sum P_G$ (MW)			**3787.9707**	**3801.0322**	**3798.5737**	**3799.1003**	**3803.5565**	**3795.5089**
CPU time (s)			1565	2849	1844	2156	2583	**1987**

V. TEST SYSTEM 2: MODIFIED ALGERIAN POWER SYSTEM DZA 114-BUS

A. RESULTS OF MODIFIED DZA 114-BUS POWER SYSTEM

To evaluate applicability of the proposed techniques on the large-scale and practical power system, the modified Algerian electricity grid DZA 114-bus[31] has been considered as test system. Algerian network topology is illustrated in Figure 13 (Annex). System consists of 175 transmission-lines, which sixteen branches are equipped with tap-changing transformers, and fifteen generators. The total-load demand is (3727+ j 2070) p.u at 100 MVA base.

The slack-bus is Bus no 4. The modification is to insert two wind generators at buses #52 and #83 along with one solar generator at bus #109. All data of test system "MATPOWER format" are free only for referees. Therefore, there are a total of 46 variables to be optimized, including 15 active power of generators, 15 voltage magnitudes of generators, and sixteen tap-changer adjustment. Also, this power system exhibits undesirable voltage drops at some buses, making it harder to ensure the feasibility of solutions, especially reactive power generators. Minimum and maximum operating limits of the control variables are given in the table of results

In this part, the adopted objective-function is the total generation cost minimization by means of the SMA, GTO, HGS, AEO and OPA algorithms. Fig. 10 shows the convergence

TABLE 8. Solution of optimal power flow of case 3 for DZA 114-bus system.

Control variables	Limits		SMA	SMA		
	MIN	MAX	Case 1	Case5-a	Case5-b	Case5-c
P_{TG4}	135	1350	413.2914	417.7622	436.3025	453.7025
P_{TG5}	135	1350	411.7038	420.1827	437.6323	450.1358
P_{TG11}	10	100	100	99.8734	99.9996	100
P_{TG15}	30	300	177.3124	152.9599	182.8524	191.7323
P_{TG17}	135	1350	392.3503	488.7547	422.3965	446.5422
P_{TG19}	34.5	345	169.5086	191.8366	186.2374	195.4546
P_{TG22}	34.5	345	165.9908	219.5912	183.4647	191.4279
P_{WG52}	0	345	344.9997	249.8669	282.9889	200.8625
P_{TG80}	34.5	345	158.0744	175.8306	191.2124	197.5297
P_{WG83}	0	300	299.9990	242.7596	192.6908	174.6617
P_{TG98}	30	300	162.2803	133.7876	175.6840	189.2058
P_{TG100}	60	600	600	599.8956	600	600
P_{TG101}	20	200	200	199.9249	200.0000	199.9784
P_{TG109}	0	100	100	99.9934	99.9969	100
P_{TG111}	10	100	99.9982	99.8807	99.9968	100
V_{G4}	0.9	1.1	1.0979	1.0370	1.0219	1.0235
V_{G5}	0.9	1.1	1.0909	1.0189	1.0127	1.0152
V_{G11}	0.9	1.1	1.100	1.0458	1.0114	1.0106
V_{G15}	0.9	1.1	1.0989	1.0244	1.0122	1.0301
V_{G17}	0.9	1.1	1.0879	1.0947	1.0617	1.0411
V_{G19}	0.9	1.1	1.0629	1.0991	1.0345	0.9792
V_{G22}	0.9	1.1	1.0783	1.0803	1.0393	0.9938
V_{G52}	0.9	1.1	1.1000	1.0641	1.0943	1.0091
V_{G80}	0.9	1.1	1.0448	1.0486	1.0497	1.0361
V_{G83}	0.9	1.1	1.0813	1.0833	1.0900	1.0733
V_{G98}	0.9	1.1	1.0897	1.0879	1.0832	1.0692
V_{G100}	0.9	1.1	1.1000	1.1000	1.0997	1.0921
V_{G101}	0.9	1.1	1.0989	1.1000	1.0860	1.0662
V_{G109}	0.9	1.1	1.0991	1.1000	1.0902	1.0610
V_{G111}	0.9	1.1	1.0585	1.0893	1.0694	1.0602
F_{Cost} ($/h)			16693.11	19914.282	20101.03	20417.605
$\sum P_G$ (MW)			**3795.5089**	**3792.9**	**3791.455**	**3791.2334**
VD (p.u)			5.3316	4.4643	3.7698	2.7259
Ploss (MW)			68.5089	65.90	64.4553	64.2333

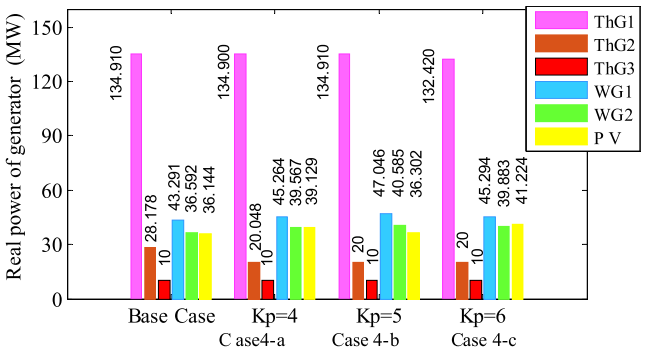

FIGURE 9. Variation of optimal scheduled real-power against reserve cost coefficients.

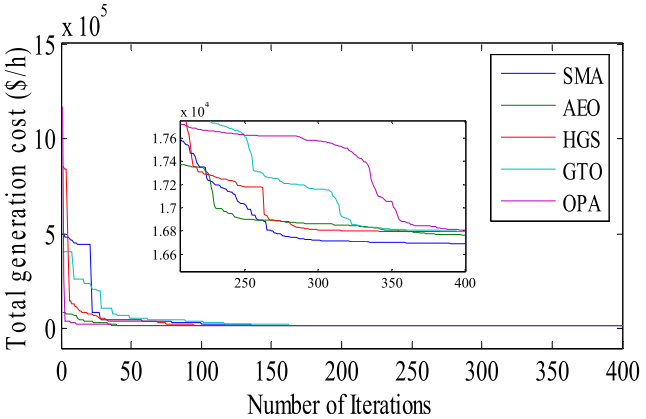

FIGURE 10. Convergence curves of different optimization techniques for DZA114-bus-case1.

curves of the considered optimizers and, as noticeably, the SMA converges to high quality solutions in the first quarter of iterations.

Based on the convergence plot presented in Fig. 10, it can be seen that SMA achieves the minimum value of generation cost compared with other optimization techniques.

Base case denotes the simulation without considering renewable energy sources, i.e., all power plants are the conventional power generators, and minimum values of active powers at buses #52, #83, and #109 are 34.5 MW, 30 MW, and 10 MW, respectively. In this case study, min-

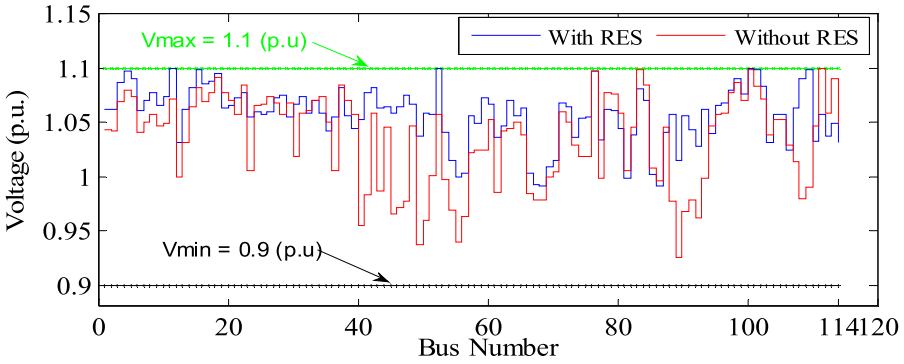

FIGURE 11. Solution of Voltage profile for both cases of DZA 114-bus Test system.

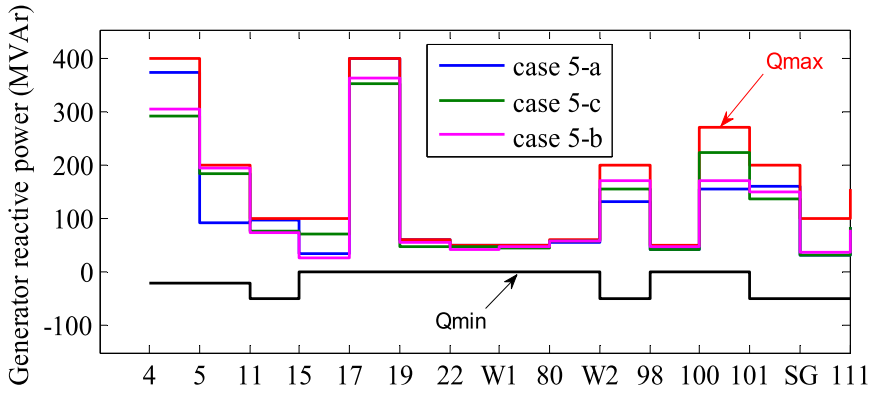

FIGURE 12. Schedule of generator reactive power for case 5 of DZA 114-bus.

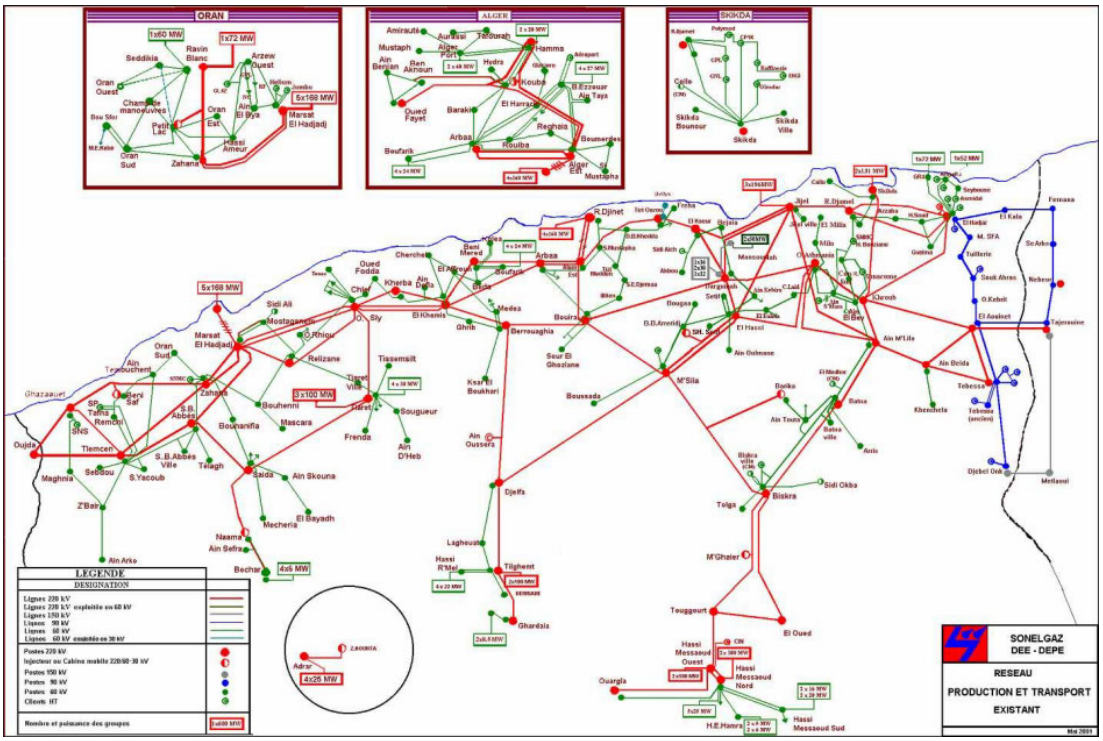

FIGURE 13. Algerian electricity grid DZA 114-bus.

imization of total generation cost is performed and the obtained results were listed in the first column of Table 7 below. Moreover, by observing the reactive power limits (Q) provided in Table 7, generators TG5, TG19, TG22, TG98,

TG98, WG52, and WG83 operate at their maximum limits of Q capacity for both cases. So, it is more necessary to regard the constraints on generators reactive power during implementation of any optimization method. Thus, from all results obtained so far, it is sufficient to highlight effectiveness of the proposed constraint handling-technique, that guarantee the feasibility of solutions, even with the real power system.

1) CASE 5 – OPTIMIZED COST AGAINST RESERVE-COST TO ALGERIAN POWER SYSTEM DZA114-BUS

In this case, scenario of case 3 is performed for DZA 114- power system. The coefficients of wind generators and solar photovoltaic unit are varied by a discrete-step of 1 starting from 6 to 8, i.e., = 6, (case 5-a), = 7, (case 5-b) = 8, (case 5-c). The penalty-cost-coefficients for all intermittent sources are remain the same as the first case. The optimal power scheduled of generators is provided in Table 8.

In this case study, increasing the coefficient of reserve cost results in a decreased contribution of wind and solar generators gradually, making in a shortage of scheduled power. So, an amount of spinning reserve is urgently needed to fill this shortage.

This shortage in power (MW) automatically compensated by thermal-generators which result in increasing the cost of thermal power generators due to the increase of the output power as observed in Table 8. Moreover, from Table 8, It can observe that active power output at slack bus for each three case 5-a, case 5-b and case 5-c increases to cover that shortage, meanwhile, output of renewable generators WG1 decrease from 350 mw to 200.86 MW and WG2 decrease from 300 MW to 174.66 MW for case 5-c. What equal to 270 MW should be compensate from thermal generators in an effort to maintaining power system stability. On the other hand, the output of solar generator is remains fix at 100 MW for three subcases, this is can be justify by technical aspect, i.e., for keeping each bus voltage magnitudes located near to the SG bus (#109) within the admissible limits [0.9-1.1] p.u. Fig. 12 presents generator reactive power scheduled for case 5 of DZA 114-bus

VI. CONCLUSION

In this article, an efficient and robust Slime Mould-inspired algorithm has been suggested for provide an optimal-solution of the stochastic OPF problem in the modified IEEE 30-bus test system and Algerian electrical network DZA 114-bus. Uncertainty nature of both solar and wind energy sources has been modelled based on the Weibull and lognormal PDFs distribution, respectively. To investigate the performance of SM algorithm, four optimization techniques: HGS, AEO, GTO, and orca predation algorithm- (OPA) are applied on different test systems. Numerical results of SMA are compared with the results found by aforementioned algorithms and other ones provided in literature. The results revealed that the SMA significantly gives a superior solution, while insuring the feasibility of solutions, where outperformed AEO, JS, HGS, MFO, GTO and BMO methods in the base case and other sub-cases whatever the constraints of test system. The results suggest that the proposed SMA can be successfully applied to solve highly nonlinear problems. The findings of this document are likely to be beneficial to researchers. Therefore, the proposed algorithm based SM technique with the superiority of feasible solutions method it is an excellent and highly recommended technique for the stochastic OPF problem, since it more efficient even in the case of practical electrical network.

ACKNOWLEDGMENT

The authors would like to acknowledge the financial support received from Taif University Researchers Supporting Project Number TURSP-2020/34, Taif University, Taif, Saudi Arabia, and in the Supporting Research Project PRFU, under Grant (A01L07UN100120210002) from the University of Bouira in Algeria.

REFERENCES

[1] P. P. Biswas, P. N. Suganthan, and G. A. J. Amaratunga, "Optimal power flow solutions incorporating stochastic wind and solar power," *Energy Convers. Manage.*, vol. 148, pp. 1194–1207, Sep. 2017.
[2] A. J. Santos and G. R. M. Da Costa, "Optimal-power-flow solution by Newton's method applied to an augmented Lagrangian function," *IEE Proc.-Gener., Transmiss. Distrib.*, vol. 142, no. 1, pp. 33–36, 1995.
[3] M. Bjelogrlic, M. S. Calovic, P. Ristanovic, and B. S. Babic, "Application of Newton's optimal power flow in voltage/reactive power control," *IEEE Trans. Power Syst.*, vol. 5, no. 4, pp. 1447–1454, Nov. 1990.
[4] H. Habibollahzadeh, G. X. Luo, and A. Semlyen, "Hydrothermal optimal power flow based on a combined linear and nonlinear programming methodology," *IEEE Trans. Power Syst.*, vol. 4, no. 2, pp. 530–537, May 1989.
[5] J. A. Momoh and J. Z. Zhu, "Improved interior point method for OPF problems," *IEEE Trans. Power Syst.*, vol. 14, no. 3, pp. 1114–1120, Aug. 1999.
[6] V. H. Hinojosa and R. Araya, "Modeling a mixed-integer-binary small-population evolutionary particle swarm algorithm for solving the optimal power flow problem in electric power systems," *Appl. Soft Comput.*, vol. 13, no. 9, pp. 3839–3852, 2013.
[7] R. P. Singh, V. Mukherjee, and S. P. Ghoshal, "Particle swarm optimization with an aging leader and challengers algorithm for the solution of optimal power flow problem," *Appl. Soft Comput.*, vol. 40, pp. 161–177, Mar. 2016.
[8] A.-A. A. Mohamed, Y. S. Mohamed, A. A. M. El-Gaafary, and A. M. Hemeida, "Optimal power flow using moth swarm algorithm," *Electr. Power Syst. Res.*, vol. 142, pp. 190–206, Jan. 2017.
[9] N. Amjady, H. Fatemi, and H. Zareipour, "Solution of optimal power flow subject to security constraints by a new improved bacterial foraging method," *IEEE Trans. Power Syst.*, vol. 27, no. 3, pp. 1311–1323, Aug. 2012.
[10] H. R. E. H. Bouchekara, M. A. Abido, and M. Boucherma, "Optimal power flow using teaching-learning-based optimization technique," *Electr. Power Syst. Res.*, vol. 114, pp. 49–59, Sep. 2014.
[11] A. E. Chaib, H. R. E. H. Bouchekara, R. Mehasni, and M. A. Abido, "Optimal power flow with emission and non-smooth cost functions using backtracking search optimization algorithm," *Int. J. Elect. Power Energy Syst.*, vol. 81, pp. 64–77, Oct. 2016.
[12] H. R. E. H. Bouchekara, A. E. Chaib, M. A. Abido, and R. A. El-Sehiemy, "Optimal power flow using an improved colliding bodies optimization algorithm," *Appl. Soft Comput.*, vol. 42, pp. 119–131, May 2016.
[13] W. Warid, "Optimal power flow using the AMTPG-Jaya algorithm," *Appl. Soft Comput.*, vol. 91, Jun. 2020, Art. no. 106252.
[14] A. K. Das, R. Majumdar, B. K. Panigrahi, and S. S. Reddy, "Optimal power flow for Indian 75 bus system using differential evolution," in *Proc. 2nd Int. Conf. (SEMCCO)*, vol. 7076, Dec. 2011, pp. 110–118.
[15] E. E. Elattar and S. ElSayed, "Modified Jaya algorithm for optimal power flow incorporating renewable energy sources considering the cost, emission, power loss and voltage profile improvement," *Energy*, vol. 178, pp. 598–609, Jul. 2019.

[16] P. P. Biswas, P. N. Suganthan, R. Mallipeddi, and G. A. J. Amaratunga, "Optimal power flow solutions using differential evolution algorithm integrated with effective constraint handling techniques," *Eng. Appl. Artif. Intell.*, vol. 68, pp. 81–100, Feb. 2018.
[17] E. E. Elattar, "Optimal power flow of a power system incorporating stochastic wind power based on modified moth swarm algorithm," *IEEE Access*, vol. 7, pp. 89581–89593, 2019.
[18] Z. Ullah, S. Wang, J. Radosavljević, and J. Lai, "A solution to the optimal power flow problem considering WT and PV generation," *IEEE Access*, vol. 7, pp. 46763–46772, 2019.
[19] Y.-C. Chang, T.-Y. Lee, C.-L. Chen, and R.-M. Jan, "Optimal power flow of a wind-thermal generation system," *Int. J. Elect. Power Energy Syst.*, vol. 55, pp. 312–320, Feb. 2014.
[20] C. Mishra, S. P. Singh, and J. Rokadia, "Optimal power flow in the presence of wind power using modified cuckoo search," *IET Gener., Transmiss. Distrib.*, vol. 9, no. 7, pp. 615–626, Apr. 2015.
[21] S. S. Reddy, "Optimal scheduling of thermal-wind-solar power system with storage," *Renew. Energy*, vol. 101, pp. 1357–1368, Feb. 2017.
[22] S. Li, H. Chen, M. Wang, A. A. Heidari, and S. Mirjalili, "Slime mould algorithm: A new method for stochastic optimization," *Future Gener. Comput. Syst.*, vol. 111, pp. 300–323, Oct. 2020.
[23] M. H. Sulaiman and Z. Mustaffa, "Optimal power flow incorporating stochastic wind and solar generation by Metaheuristic optimizers," *Microsyst. Technol.*, vol. 27, no. 9, pp. 3263–3277, Sep. 2021.
[24] K. Deb, "An efficient constraint handling method for genetic algorithms," *Comput. Methods Appl. Mech. Eng.*, vol. 186, nos. 2–4, pp. 311–338, 2000.
[25] A. D. Sappa and F. Dornaika, "An edge-based approach to motion detection," in *Computational Science*, vol. 11538. Berlin, Germany: Springer, May 2019.
[26] C. A. C. Coello, "Theoretical and numerical constraint-handling techniques used with evolutionary algorithms: A survey of the state of the art," *Comput. Methods Appl. Mech. Eng.*, vol. 191, pp. 1245–1287, Jan. 2002.
[27] I. U. Khan, N. Javaid, K. A. A. Gamage, C. J. Taylor, S. Baig, and X. Ma, "Heuristic algorithm based optimal power flow model incorporating stochastic renewable energy sources," *IEEE Access*, vol. 8, pp. 148622–148643, 2020.
[28] R. D. Zimmerman, C. E. Murillo-Sánchez, and R. J. Thomas, "MATPOWER: Steady-state operations, planning, and analysis tools for power systems research and education," *IEEE Trans. Power Syst.*, vol. 26, no. 1, pp. 12–19, Feb. 2011.
[29] M. H. Hassan, S. Kamel, M. A. El-Dabah, T. Khurshaid, and J. L. Dominguez-Garcia, "Optimal reactive power dispatch with time-varying demand and renewable energy uncertainty using Rao-3 algorithm," *IEEE Access*, vol. 9, pp. 23264–23283, 2021.
[30] M. Farhat, S. Kamel, A. M. Atallah, and B. Khan, "Optimal power flow solution based on jellyfish search optimization considering uncertainty of renewable energy sources," *IEEE Access*, vol. 9, pp. 100911–100933, 2021.
[31] S. Mouassa, F. Jurado, T. Bouktir, and M. A. Z. Raja, "Novel design of artificial ecosystem optimizer for large-scale optimal reactive power dispatch problem with application to Algerian electricity grid," *Neural Comput. Appl.*, vol. 33, no. 13, pp. 7467–7490, Jul. 2021.
[32] S. Li, W. Gong, L. Wang, X. Yan, and C. Hu, "Optimal power flow by means of improved adaptive differential evolution," *Energy*, vol. 198, May 2020, Art. no. 117314.

SOUHIL MOUASSA was born in Ziama Mansouriah, Jijel, Algeria. He received the B.S. and master's degrees in electrical engineering from the University of Setif, Algeria, in 2009 and 2012, respectively, and the Ph.D. degree from the University of Jaén, Jaén, Spain, and Sétif 1 University, in 2021. He is currently an Associate Professor at the University of Bouira, Algeria. He is also a researcher between both universities. His primary research interests include optimal power system planning and operation, unconventional methods for power system analysis, micro-grids planning and operation, renewable energy, demand side management, and smart homes. He works as an Expert Reviewer of IEEE Access.

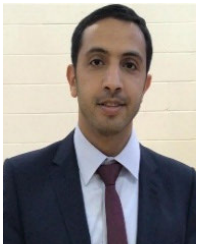

AHMED ALTHOBAITI (Member, IEEE) received the B.S. degree in electrical engineering from Umm Al-Qura University, Makkah, in 2006, the M.Sc. degree in electrical power from the School of Electrical and Electronic Engineering, Newcastle University, in 2011, and the Ph.D. degree in electrical engineering from Newcastle University, in 2018. He is currently an Assistant Professor of electrical engineering with Taif University, Saudi Arabia. His research interests include electric current control, electric motors, electric vehicles, robotics, fault diagnosis, internal combustion engines, power capacitors, and non-linear systems.

FRANCISCO JURADO (Senior Member, IEEE) was born in Linares, Jaén, Spain. He received the M.Sc. and Dr.Ing. degrees from the National University of Distance Education, Madrid, Spain, in 1995 and 1999, respectively. Since 1985, he has been a Professor with the Department of Electrical Engineering, University of Jaén, Jaén. His current research interests include power systems, modeling, and renewable energy.

SHERIF S. M. GHONEIM (Senior Member, IEEE) received the B.Sc. and M.Sc. degrees from the Faculty of Engineering at Shoubra, Zagazig University, Egypt, in 1994 and 2000, respectively, and the Ph.D. degree in electrical power and machines from the Faculty of Engineering, Cairo University, in 2008. Since 1996, he has been a Lecturer with the Faculty of Industrial Education, Suez Canal University, Egypt. From 2005 to 2007, he was a Guest Researcher with the Institute of Energy Transport and Storage (ETS), University of Duisburg–Essen, Germany. He joined the Department of Electrical Engineering, Faculty of Engineering, Taif University, as an Associate Professor. His research interests include grounding systems, breakdown in SF6 gas, dissolved gas analysis, and AI technique applications.